



# 1 **High bacterial organic carbon uptake in the Eastern Tropical**

## 2 **South Pacific oxygen minimum zone**

3 Marie Maßmig, Jan Lüdke, Gerd Krahnemann, Anja Engel\*

4 GEOMAR Helmholtz Centre for Ocean Research Kiel, Düsternbrooker Weg 20, D-24105 Kiel, Germany

5 *Correspondence to:* Anja Engel (aengel@geomar.de)

6 **Abstract.** Oxygen minimum zones (OMZs) show distinct biogeochemical processes that relate to microorganisms  
7 being able to thrive under low or even absent oxygen. Microbial degradation of organic matter is expected to be  
8 reduced in OMZs, although quantitative evidence is low. Here, we present heterotrophic bacterial production (<sup>3</sup>H  
9 leucine-incorporation), extracellular enzyme rates (leucine aminopeptidase /β-glucosidase) and bacterial cell  
10 abundance for various *in situ* oxygen concentrations in the water column of the Eastern Tropical South Pacific off  
11 Peru. Bacterial heterotrophic activity in the suboxic core of the OMZ (at *in situ* ≤5 μmol O<sub>2</sub> kg<sup>-1</sup>) ranged from 0.6 to  
12 160 μmol C m<sup>-3</sup> d<sup>-1</sup> and was not significantly lower than in waters of 5-60 μmol O<sub>2</sub> kg<sup>-1</sup>. Moreover, bacterial  
13 abundance in the OMZ was slightly and leucine aminopeptidase activity even significantly higher in suboxic waters  
14 compared to the upper oxycline suggesting no impairment of bacterial organic matter degradation in the core of the  
15 OMZ. Nevertheless, high cell-specific bacterial production and extracellular enzyme rates were observed in samples  
16 from the upper or lower oxyclines corroborating earlier findings of highly active and distinct micro-aerobic bacterial  
17 communities. To assess the impact of bacterial degradation of dissolved organic matter for oxygen loss in the  
18 Peruvian OMZ, we compared diapycnal fluxes of oxygen and dissolved organic carbon (DOC) and their microbial  
19 uptake within the upper 60m of the water column. Our data indicate bacterial growth efficiencies of 0.5-8.6% at the  
20 upper oxycline, resulting in a high bacterial oxygen demand that can explain up to 33% of the observed average  
21 oxygen loss over depth. Our study therewith shows that microbial degradation of DOM has a considerable share in  
22 sustaining the OMZ off Peru.



## 23 1. Introduction

24 In upwelling zones at eastern continental margins, oxygen minimum zones (OMZs) with hypoxic ( $<60 \mu\text{mol O}_2 \text{ kg}^{-1}$ )  
25 <sup>1</sup>), suboxic ( $<5 \mu\text{mol O}_2 \text{ kg}^{-1}$ ) or even anoxic conditions occur (Gruber, 2011; Thamdrup et al., 2012). OMZs have  
26 expanded over the past years resulting in an  $\sim 3.7\%$  increase of hypoxic waters at depth (200 dbar) between 1960 and  
27 2008 (Stramma et al., 2010). One of the largest anoxic water masses in the global ocean ( $2.4 \times 10^{13} \text{ m}^3$ ) is located in  
28 the Eastern Tropical South Pacific and includes the Peruvian upwelling system (Kämpf and Chapman, 2016;  
29 Thamdrup et al., 2012). There, nutrient-rich water is upwelled and supports high rates of primary production and  
30 organic matter accumulation. Biological degradation of organic matter subsequently reduces oxygen below the  
31 surface mixed layer (Kämpf and Chapman, 2016). As a consequence, and supported by sluggish ventilation of water  
32 masses, a permanent OMZ forms between 100 and 500 m depth, with upper and lower boundaries, i.e. oxyclines,  
33 varying within seasonal and inter-annual cycles (Czeschel et al., 2011; Graco et al., 2017; Kämpf and Chapman,  
34 2016).

35 Within OMZs, microbes apply anaerobic respiratory pathways that yield less metabolic energy compared to aerobic  
36 respiration. For instance, denitrification or dissimilatory nitrate reduction to ammonia (DNRA) result only in 99 %,  
37 or 64 % of the energy (kJ) per oxidized carbon atom that is produced by aerobic respiration (Lam and Kuypers,  
38 2011). Meanwhile, bacteria are mainly responsible for the remineralization of organic matter into nutrients and  
39 carbon dioxide ( $\text{CO}_2$ ) in the ocean (Azam et al., 1983). Thus, microbial activity and consequently organic matter  
40 remineralization in anoxic waters might be reduced, possibly explaining observations of enhanced vertical carbon  
41 export in OMZ regions (Devol and Hartnett, 2001; Roullier et al., 2014). As a consequence, expanding OMZs could  
42 result in increased  $\text{CO}_2$  storage in the ocean.

43 During the degradation process, low molecular weight (LMW  $<1 \text{ kDa}$ ) organic compounds can directly be taken up  
44 by bacteria (Azam et al., 1983; Weiss et al., 1991). However, in the ocean, bioavailable organic matter is commonly  
45 in the form of particulate organic matter or high molecular weight (HMW) dissolved organic matter (Benner and  
46 Amon, 2015). To access this organic matter pool, bacteria produce extracellular, substrate specific enzymes that  
47 hydrolyse polymers into LMW units (Hoppe et al., 2002). Taken-up, organic matter is partly incorporated into  
48 bacterial biomass, or respired to  $\text{CO}_2$ , which may evade to the atmosphere (Azam et al., 1983). Rates of enzymatic  
49 organic matter hydrolysis or bacterial production are controlled by the environment, i.e. temperature and pH, but can  
50 be actively regulated e.g. in response to changing organic matter supply and quality (Boetius and Lochte, 1996;  
51 Grossart et al., 2006; Pantoja et al., 2009; Piontek et al., 2014). However, the effect of oxygen concentration, which  
52 dictates the respiratory pathway and thus energy gain, on bacterial production and the expression of extracellular  
53 enzymes in aquatic systems, is poorly understood and previous results are ambiguous. For instance, volumetric rates  
54 of protein hydrolysing enzymes (peptidases) did not differ between oxic and anoxic incubations of Baltic Sea water  
55 (Hoppe et al., 1990), but were significantly higher in oxic compared to anoxic waters in Cariaco waters (Taylor et al.,  
56 2009). Bacterial production was higher in anoxic lake waters (Cole and Pace, 1995), whereas in the Pacific waters  
57 off Chile bacterial production and dissolved organic matter decomposition rates did not change in relation to oxygen  
58 concentrations (Lee, 1992; Pantoja et al., 2009). Further measurements of microbial activity such as extracellular



59 enzyme rates, the initial step of organic matter degradation (Hoppe et al., 2002), and bacterial production in OMZs  
60 are necessary to unravel possible adaptation strategies of bacterial communities to suboxic and anoxic conditions as  
61 for instance high extracellular enzyme rates compensating a putative lower efficiency of anaerobic respiration and  
62 the subsequent biogeochemical effects. Especially, combined investigations of extracellular enzymatic rates,  
63 bacterial production (measured by  $^3\text{H}$  leucine-incorporation) and carbon fluxes sampled at various *in situ* oxygen  
64 concentrations are still missing. These data, however, are crucial to inform ocean biogeochemical models that aim at  
65 quantification of  $\text{CO}_2$  uptake and nitrogen loss processes in oxygen depleted areas.

66 We studied bacterial degradation of organic matter in the OMZ off Peru during an extensive sampling campaign in  
67 the Austral winter 2017. We determined rates of total and cell-specific bacterial production ( $^3\text{H}$  leucine-  
68 incorporation) as well as of leucine aminopeptidase (LAPase) and  $\beta$ -glucosidase (GLUCase). We estimate bacterial  
69 utilisation of dissolved organic carbon (DOC) supplied by diapycnal transport into the OMZ and discuss the  
70 contribution of bacterial degradation activity to the formation and persistence of the OMZ off Peru.

## 71 **2. Methods**

### 72 **2.1. Study site and CTD measurements**

73 Samples were taken during the cruises M136 and M138 on the R/V METEOR off Peru in April and June 2017,  
74 respectively (Fig. 1). Seawater was sampled with 24 Niskin bottles (10 L) on a general oceanic rosette system. At  
75 each station, 5 to 11 depths were sampled between 3 and 800 m (supplementary Table 1). Oxygen concentrations,  
76 temperature and depth were measured with a Sea-Bird SBE 9-plus CTD System (Sea-Bird Electronics, Inc., USA).  
77 Oxygen concentrations at each depth were determined with a SBE 43 oxygen sensor, calibrated with Winkler  
78 titrations (Winkler, 1888), resulting in an overall accuracy of  $1.5 \mu\text{mol kg}^{-1}$  oxygen. Chlorophyll *a* fluorescence was  
79 detected with a WETStar chlorophyll *a* sensor (WET Labs, USA) and converted to  $\mu\text{g l}^{-1}$  using factors given by the  
80 manufacturer (Wetlabs).

### 81 **2.2. Dissolved organic carbon, total dissolved nitrogen, dissolved hydrolysable amino** 82 **acids and dissolved high molecular weight carbohydrates**

83 DOC and total dissolved nitrogen (TDN) samples were taken at all stations, whereas the further analysis of DOC  
84 data was limited to stations with compatible bacterial production data and turbulence measurements (stations G-T).  
85 For DOC and TDN 20 ml of seawater was sampled in replicates, whereas both replicates were only analysed in case  
86 of conspicuous data. Samples were filtered through a syringe filter ( $0.45 \mu\text{m}$  glass microfiber GD/X membrane,  
87 Whatman <sup>TM</sup>), rinsed with 50 ml sample, into a combusted glass ampoule (8 h,  $500 \text{ }^\circ\text{C}$ ). Before sealing the ampoules,  
88  $20 \mu\text{l}$  of 30 % ultrapure hydrochloric acid were added. Samples were stored at  $4 \text{ }^\circ\text{C}$  in the dark for 3 months until  
89 analyses. DOC and TDN were analysed using a TOC-VCSH with a TNM-1 detector (Shimadzu), applying a high-  
90 temperature catalytic oxidation method modified from Sugimura and Suzuki (1988). The instrument was calibrated  
91 with potassium hydrogen phthalate standard solutions ( $0$  to  $416.7 \mu\text{mol C l}^{-1}$ ) (Merck 109017) and a potassium  
92 nitrate standard solution ( $0$ - $57.1 \mu\text{mol N l}^{-1}$ ) (Merck 105065). The instrument blank was examined with reference  
93 seawater standards (Hansell laboratory RSMAS University of Miami). The relative standard deviation (RSD)



94 between repeated measurements is <1.1 % and <3.6 % and the detection limit is  $1 \mu\text{mol l}^{-1}$  and  $2 \mu\text{mol l}^{-1}$  for DOC  
95 and TDN, respectively.

96 At each station replicate 6 ml and 20 ml sample for the analysis of dissolved amino acids (DHAA) and dissolved  
97 combined carbohydrates (DCHO) were filtered through rinsed Acrodisc® 0.45 $\mu\text{m}$  GHP membrane (Pall) and stored  
98 in combusted vials (8 h, 500 °C) at -20 °C, respectively. Replicates were only analysed, if the first sample analyses  
99 resulted conspicuous data. The following DHAA were analysed: Alanine, Arginine, Glycine, Leucine,  
100 Phenylalanine, Serine, Threonine, Tyrosine, Valine, Aspartic acid + Asparagine (co-eluted), Glutamine + Glutamic  
101 acid (co-eluted),  $\gamma$ -Aminobutyric acid and Isoleucine. DHAA samples were analysed with a high performance liquid  
102 chromatograph (1260 HPLC system, Agilent Technologies) using a  $\text{C}_{18}$  column (Phenomex Kinetex) after in line  
103 ortho-phthaldialdehyde derivatization with mercaptoethanol after Lindroth and Mopper (1979) and Dittmar et al.  
104 (2009) with slight modifications after Engel and Galgani (2016). DCHO samples were desalted by membrane  
105 dialysis (1kDa, Spectra Por) and analysed with a high performance anion exchange chromatography (HPAEC)  
106 (DIONEX ICS3000DC) after Engel and Händel (2011).

### 107 **2.3. Diapycnal fluxes of oxygen and dissolved organic carbon**

108 In this study, we calculated DOC and oxygen loss rates ( $\text{mmol m}^{-3} \text{d}^{-1}$ ) from the changes in diapycnal fluxes over  
109 depth. Therefore, oxygen and DOC profiles were used (stations G-T), excluding the mixed layer, defined by  
110 temperature deviating  $\leq 0.2^\circ\text{C}$  from the maximum, but excluding at least the upper 10 m. The diapycnal flux ( $\Phi_S$ )  
111 was calculated for each CTD profile (Fischer et al., 2013; Schafstall et al., 2010) assuming a constant gradient  
112 between two sampled depths for DOC and oxygen:

$$113 \quad 1. \quad \Phi_S = -K_\rho \nabla C_S$$

114 where  $\nabla C_S$  is the gradient ( $\text{mol m}^{-4}$ ). The diapycnal diffusivity of mass ( $K_\rho$ ) ( $\text{m}^2 \text{s}^{-1}$ ) was assumed to be constant  
115 ( $10^{-3} \text{m}^2 \text{s}^{-1}$ ), which is reasonable compared with turbulence measurements by a freefalling microstructure probe  
116 (see Fig. 5 and supplementary). DOC loss rates ( $\nabla \Phi_{\text{DOC}}$ ;  $\text{mmol m}^{-3} \text{d}^{-1}$ ) and oxygen loss rates ( $\nabla \Phi_{\text{DO}}$ ;  $\text{mmol m}^{-3} \text{d}^{-1}$ )  
117 were assumed to be equal to the negative vertical divergence of  $\Phi_S$  calculated from the mean diapycnal flux profile,  
118 implying all other physical supply processes to be negligible.

### 119 **2.4. Bacterial abundance**

120 Bacterial abundance was sampled in replicates at each station, whereas replicates were only analysed in exceptions.  
121 Abundance was determined by flow cytometry after Gasol and Del Giorgio (2000) from 1.6 ml sample, fixed with  
122 0.75 $\mu\text{l}$  25 % glutaraldehyde on board and stored at -80°C for maximal 3 month until analyses. Prior to analysis  
123 samples were thawed and 10  $\mu\text{L}$  Flouresbrite® fluorescent beads (Polyscience, Inc.) and 10  $\mu\text{L}$  Sybr Green  
124 (Invitrogen) (final concentration: 1x of the 1000x Sybr Green concentrate) were added to 400  $\mu\text{l}$  sample. Cells were  
125 counted on a FACS Calibur (Becton Dickinson), calibrated with TruCount Beads™ (BD) with a measurement error  
126 of 2 % RSD.



## 127            **2.5. Bacterial production, oxygen demand and growth efficiency**

128        For bacterial production, the incorporation of radioactive labelled leucine ( $^3\text{H}$ ) (specific activity  $100 \text{ Ci mmol}^{-1}$ ,  
129        Biotrend) was measured (Kirchman et al., 1985; Smith and Azam, 1992) at all depths of stations G-T as replicates.  
130        For this, the radiotracer at a saturating final concentration of  $20 \text{ nmol l}^{-1}$  was added to 1.5 ml of sample and incubated  
131        for 3 hours in the dark at  $13^\circ\text{C}$ . Controls were poisoned with trichloroacetic acid. Samples were measured with a  
132        liquid scintillation counter (Hidex 300 SL, Triathaler<sup>TM</sup>, FCI). Samples taken at *in situ* oxygen concentrations of  $< 5$   
133         $\mu\text{mol kg}^{-1}$  were incubated under anoxic conditions by gentle bubbling with gas (0.13 %  $\text{CO}_2$  in pure  $\text{N}_2$ ). Samples  
134        from oxic waters were incubated with head space, without bubbling. All samples were shaken thoroughly in  
135        between, therefore the bubbling of just one treatment won't have any effect.  $^3\text{H}$ -leucine uptake was converted to  
136        carbon units applying a conversion factor of  $1.5 \text{ kg C mol}^{-1}$  leucine (Simon and Azam, 1989). An analytical error of  
137        5.2 % RSD was estimated with triplicate calibrations. Samples with a s.d. (standard deviation)  $> 30\%$  between  
138        replicates were excluded.

139        The BOD is the amount of oxygen needed to fully oxygenize DOC that has been taken up and not transformed into  
140        biomass by bacterial production (BP). The BOD was calculated as the difference between the estimated bacterial  
141        DOC uptake and the bacterial production (BP) applying a respiratory quotient (*cf*) of 1 (Eq. (2)) (Del Giorgio and  
142        Cole, 1998).

$$143 \qquad \qquad \qquad 2. \quad \text{BOD} = (\text{DOC uptake} - \text{BP}) \times cf$$

144        The DOC uptake was calculated with two different assumptions: i) the DOC uptake by bacteria equals the DOC loss  
145        rate or ii) the bacterial growth efficiency (BGE) follows the established temperature dependence, resulting in a BGE  
146        between 0.1 and 0.3 in the depth range of 10-60 m and an *in situ* temperature that varied between  $14$  and  $19^\circ\text{C}$   
147        (Rivkin and Legendre, 2001) and can be used to estimate the bacterial DOC uptake (Eq. (3)).

$$148 \qquad \qquad \qquad 3. \quad \text{microbial DOC uptake} = \frac{\text{BP}}{\text{BGE}}$$

## 149            **2.6. Extracellular enzyme rates**

150        Potential hydrolytic rates of LAPase and GLUCase were determined with fluorescent substrate analogues (Hoppe,  
151        1983). L-leucine-7-amido-4-methylcoumarin (Sigma Aldrich) and 4-methylumbelliferyl- $\beta$ -D-glucopyranoside  
152        (Acros Organics) were added in final concentrations of 1, 5, 10, 20, 50, 80, 100 and  $200 \mu\text{mol l}^{-1}$  in black 69 well  
153        plates (Costar) and kept frozen for at most one day until replicates of  $200 \mu\text{l}$  sample were added. After 0 and 12  
154        hours of incubation at  $13^\circ\text{C}$  in the dark, fluorescence was measured with a plate reader fluorometer (FLUOstar  
155        Optima, BMG labtech) (excitation: 355 nm; emission: 460 nm). An error of 2 % RSD was defined using the  
156        calibration with triplicates. Blanks with MilliQ were performed to exclude an increase in substrate decay over time.

157        Samples were collected in replicates ( $n=2$ ) at station A-K and incubated directly after sampling under oxygen  
158        conditions resembling *in situ* oxygen conditions. For samples  $> 5 \mu\text{mol in situ O}_2 \text{ kg}^{-1}$  incubations were conducted  
159        under atmospheric oxygen conditions. Samples  $< 5 \mu\text{mol in situ O}_2 \text{ kg}^{-1}$  were incubated in a gas tight incubator that



160 was filled with N<sub>2</sub>, to reduce oxygen concentrations (8 to 40 μmol O<sub>2</sub> kg<sup>-1</sup>). To investigate the influence of the  
161 different incubation methods we additionally incubated samples > 5 μmol *in situ* O<sub>2</sub> kg<sup>-1</sup> under reduced oxygen  
162 concentrations. On average incubations under reduced oxygen concentration yielded 2-27% higher values than those  
163 incubated under atmospheric oxygen conditions. However, the observed trends over depth remained similar (see  
164 supplementary discussion and supplementary Fig. 1).

165 Calibration was conducted with 7-amino-4-methylcoumarin (2 nmol l<sup>-1</sup> to 1 μmol l<sup>-1</sup>) (Sigma Aldrich) and 4-  
166 methylumbelliferone (Sigma Aldrich) (16 nmol l<sup>-1</sup> to 1 μmol l<sup>-1</sup>) in seawater at atmospheric oxygen concentrations  
167 and under N<sub>2</sub> atmosphere.

168 Maximum reaction velocity (V<sub>max</sub>) at saturating substrate concentrations was calculated using both replicates at once,  
169 with the simple ligand binding function in SigmaPlot™ 12.0 (Systat Software Inc., San Jose, CA). Values for V<sub>max</sub>  
170 with a s.d. >30 % were excluded from further analyses. The degradation rate (δ) [μmol C m<sup>-3</sup> d<sup>-1</sup>] of DHAA by  
171 LAPase and DCHO by GLUCase was calculated after Piontek et al. (2014):

172 
$$4. \quad \delta = \frac{h_r + c}{100}$$

173 where  $h_r$  [% d<sup>-1</sup>] is the hydrolyses turnover at 10 μmol l<sup>-1</sup> substrate concentration and  $c$  is the carbon content of  
174 DHAA [μmol C m<sup>-3</sup>]. Measurements of  $h_r$  with a s.d. between duplicates of more than 30% were excluded. The same  
175 procedure was conducted with the carbon content of dissolved hydrolysable leucine, instead of DHAA, to account  
176 for variations in leucine concentrations, which is the main amino acid hydrolysed by LAPase.

## 177 2.7. Data analyses

178 Data were plotted with Ocean Data View 4.74 (Schlitzer, 2016), MATLAB (8.3.0.532 (R2014a)) and R version 3.4.2  
179 using the package *ggplot2* (Hadley Wickham, 2016; R Development Core Team, 2008). Statistical significances  
180 between different regimes (see supplementary Table 2 for mean and s.d. within different regimes and main text for  
181 statistical results) were tested with a *Wilcoxon test* (W) and correlation with the *Spearman Rank correlation* (S) in R  
182 version 3.4.2 (R Development Core Team, 2008) using following R packages: *FSA*, *car* and *multcomp* (Derek H.  
183 Olge, 2018; Horthorn et al., 2008; John Fox and Sanford Weisberg, 2011). For this extracellular enzyme data of  
184 station A-K and bacterial production data of station G-T were used, since not all parameters could be sampled at all  
185 depth. Diapycnal fluxes of DOC and oxygen were calculated with MATLAB (8.3.0.532 (R2014a)) and the Toolbox  
186 Gibbs SeaWater (GSW) Oceanographic Toolbox (3.05) (McDougall and Barker, 2011).

187 Samples were categorized into different oxygen regimes. Due to sensitivities of oxygen measurements, we did not  
188 distinguish between anoxic and suboxic regimes, but defined the “OMZ” oxygen regime by a threshold ≤ 5 μmol O<sub>2</sub>  
189 kg<sup>-1</sup> (Gruber, 2011). We defined the oxycline as one regime (>5 to <60 μmol O<sub>2</sub> kg<sup>-1</sup>) or separated it into  
190 “low\_hypoxic” (>5 to <20 μmol O<sub>2</sub> kg<sup>-1</sup>) and “high\_hypoxic” (>20 to <60 μmol O<sub>2</sub> kg<sup>-1</sup>) regimes, representing  
191 important thresholds of oxygen concentrations for biological processes (Gruber, 2011). Oxygen concentrations >60  
192 μmol O<sub>2</sub> kg<sup>-1</sup> were defined as “oxic”. Moreover, we differentiated between oxygen regimes situated above and below  
193 the OMZ.



### 194 3. Results

#### 195 3.1. Biogeochemistry of the Peruvian OMZ

196 During our two cruises to the Peruvian upwelling system (Fig. 1), in April and June 2017 chlorophyll *a* (Chl *a*)  
197 reached maximum of  $8 \mu\text{g l}^{-1}$  within the upper 25 m. At depths  $>50$  m Chl *a* was generally below detection limit  
198 (Fig. 2a, exemplary stations). Oxygen  $>100 \mu\text{mol kg}^{-1}$  was observed in the surface mixed layer, decreased steeply  
199 with depth and was below detection of Winkler titration at  $>100$  m (Fig. 3a and 4a). Oxygen increased again to up to  
200  $15 \mu\text{mol kg}^{-1}$  at  $>500$  m (Fig. 3a and 4a). Temperatures ranged between 14 and  $24 \text{ }^\circ\text{C}$  in the upper 100 m and  
201 decreased to  $7 \text{ }^\circ\text{C}$  at 600 m (Fig. 2b). TDN concentrations increased with depth from 17-32  $\mu\text{mol l}^{-1}$  within the upper  
202 40 m to a maximum of  $51 \mu\text{mol l}^{-1}$  at 600 m (Fig. 2c). DOC decreased with depth from  $81 \pm 30 \mu\text{mol l}^{-1}$  at the surface  
203 to  $42 \mu\text{mol l}^{-1}$  at 600 m depth, with the steepest gradient in the upper 20-60 m (Fig. 2d).

#### 204 3.2. Bacterial production and enzymatic activity

205 Bacterial production varied strongly throughout the study region and ranged from 0.6 to  $614 \mu\text{mol C m}^{-3} \text{ d}^{-1}$  (Fig.  
206 3b), decreased in general from surface to depth (except for the most coastal stations) and showed significantly higher  
207 rates in the oxygenated surface compared to the OMZ ( $n_{\text{OMZ}}=61$ ,  $n_{\text{oxic}}=34$ ,  $p<0.01$ ,  $W=214$ ) (Fig. 3b). Bacterial  
208 production did not differ between the oxyclines and the suboxic core waters, neither off-shore (suboxic:  $0.6\text{-}91 \mu\text{mol}$   
209  $\text{C m}^{-3} \text{ d}^{-1}$ ; oxyclines:  $2\text{-}149 \mu\text{mol C m}^{-3} \text{ d}^{-1}$ ) ( $n_{\text{OMZ}}=46$ ,  $n_{\text{oxyclines}}=25$ ,  $p=0.28$ ,  $W=484$ ) nor at the most coastal stations  
210 (G and T) (suboxic:  $80\text{-}160 \mu\text{mol C m}^{-3} \text{ d}^{-1}$ ) (oxycline:  $34\text{-}195 \mu\text{mol C m}^{-3} \text{ d}^{-1}$ ) ( $n_{\text{OMZ}}=2$ ,  $n_{\text{oxycline}}=8$ ,  $p=0.4$ ,  $W=12$ ).  
211 Further, no significant correlation was observed between bacterial production and oxygen at *in situ*  $<20 \mu\text{mol O}_2 \text{ kg}^{-1}$   
212 ( $S=53904$ ,  $p=0.64$ ,  $r^2=0.06$ ,  $n=70$ ). No significant increase of bacterial production was observed below the OMZ ( $2\text{-}$   
213  $10.5 \mu\text{mol C m}^{-3} \text{ d}^{-1}$ ) compared to the core OMZ ( $0.6\text{-}160 \mu\text{mol C m}^{-3} \text{ d}^{-1}$ ) even though oxygen increased from  $<5$  to  
214  $15 \mu\text{mol kg}^{-1}$  (Fig. 3b) ( $n_{\text{OMZ}}=48$ ,  $n_{\text{bottom_low_hypoxic}}=5$ ,  $p=0.08$ ,  $W=62$ ).

215 Overall, bacterial abundance ranged from 1 to  $49 \times 10^5$  cells  $\text{ml}^{-1}$ , with highest abundance observed at the surface and  
216 close to the sediment. Cell abundance in the upper oxycline ( $3\text{-}16 \times 10^5$  cells  $\text{ml}^{-1}$ ) was statistically similar to the  
217 OMZ core ( $1\text{-}25 \times 10^5$  cells  $\text{ml}^{-1}$ ) ( $n_{\text{upper_oxycline}}=36$ ,  $n_{\text{OMZ}}=93$ ,  $p=0.86$ ,  $W=1640$ ). However, we could observe a slight  
218 accumulation of bacterial cells in the OMZ core, compared to the upper oxycline (Fig. 3c). A sharp decrease in  
219 bacterial abundance was observed below the OMZ.

220 Estimates for the *in situ* degradation rate of DHAA by LAPase take into account the available concentrations of  
221 DHAA and varied between 0.7 and  $31.2 \mu\text{mol C m}^{-3} \text{ d}^{-1}$ . LAPase degradation rates observed within the OMZ core ( $5$   
222  $\pm 1.8 \mu\text{mol C m}^{-3} \text{ d}^{-1}$ ) were significantly higher than in the upper oxycline ( $2.5 \pm 1.2 \mu\text{mol C m}^{-3} \text{ d}^{-1}$ ) ( $n_{\text{OMZ}}=41$ ,  
223  $n_{\text{upper_low_hypoxic}}=9$ ,  $p<0.001$ ,  $W=331$ ) (Fig. 4b). To exclude an influence of changing DHAA composition over depth,  
224 LAPase activity was also calculated using *in situ* concentrations of dissolved hydrolysable leucine instead of total  
225 DHAA. Degradation rates of dissolved hydrolysable leucine by LAPase ( $0.01\text{-}1.68 \mu\text{mol C m}^{-3} \text{ d}^{-1}$ ) showed the same  
226 trend with significantly higher rates in suboxic waters than in the upper oxycline ( $n_{\text{OMZ}}=41$ ,  $n_{\text{upper_low_hypoxic}}=9$ ,  $p<0.01$   
227  $W=289$ ). Thus, differences in the molecular composition of DHAA had no influence on spatial degradation patterns  
228 being higher in suboxic waters than in the upper oxycline. In contrast, degradation rates of DCHO ( $>1\text{kDa}$ ) were



229 slightly reduced within the suboxic waters ( $0.69 \pm 1.35 \mu\text{mol C m}^{-3} \text{d}^{-1}$ ) compared to the upper oxycline ( $0.76 \pm 0.51$   
230  $\mu\text{mol C m}^{-3} \text{d}^{-1}$ ) ( $n_{\text{OMZ}}=35$ ,  $n_{\text{upper\_low\_hypoxic}}=8$ ,  $p=0.054$ ,  $W=78$ ). Since degradation rates were calculated by  
231 multiplying enzyme rates and carbon concentrations of DCHO and DHAA at *in situ* depth, differences in carbon  
232 concentrations are important for further interpretation. *In situ* carbon concentrations of DHAA were similar between  
233 the OMZ core ( $0.53 \pm 0.1 \mu\text{mol C L}^{-1}$ ) and the oxycline ( $0.57 \pm 0.2 \mu\text{mol C L}^{-1}$ ) ( $n_{\text{OMZ}}=42$ ,  $n_{\text{oxycline}}=31$ ,  $p=0.3$   $W=558$ ).  
234 In contrast, *in situ* carbon concentrations of DCHO were reduced within the OMZ core ( $1.3 \pm 0.4 \mu\text{mol C L}^{-1}$ )  
235 compared to the oxycline ( $1.5 \pm 0.6 \mu\text{mol C L}^{-1}$ ) ( $n_{\text{OMZ}}=42$ ,  $n_{\text{oxycline}}=31$ ,  $p=0.01$   $W=502$ ) (Fig. 2e, f), suggesting that  
236 calculated differences between degradation rates may be influenced by different carbon concentrations. Potential  
237 hydrolytic rates at saturating substrate concentration ( $V_{\text{max}}$ ) of LAPase ranged between 7 and 168  $\text{nmol l}^{-1} \text{h}^{-1}$  and  
238 were 10 times lower for GLUCase. LAPase  $V_{\text{max}}$  was significantly higher within the suboxic waters ( $50 \pm 22 \text{nmol l}^{-1}$   
239  $\text{h}^{-1}$ ) compared to the oxycline ( $34 \pm 18 \text{nmol l}^{-1} \text{h}^{-1}$ ) ( $n_{\text{OMZ}}=49$ ,  $n_{\text{oxycline}}=26$ ,  $p<0.01$   $W=1045$ ) and GLUCase  $V_{\text{max}}$  was  
240 more similar within the suboxic waters ( $1.6 \pm 1.6 \text{nmol l}^{-1} \text{h}^{-1}$ ) compared to the oxycline ( $1.1 \pm 0.5 \text{nmol l}^{-1} \text{h}^{-1}$ ) (Fig.  
241 4d, e).

242 To investigate physiological effects of suboxia, we normalized bacterial production and enzymatic rates to cell  
243 abundance. Cell-specific production ranged between 2 and 286  $\text{amol C cell}^{-1} \text{d}^{-1}$  (Fig. 3d) and, in contrast to total  
244 production, was positively correlated to oxygen concentrations at  $<20 \mu\text{mol O}_2 \text{kg}^{-1}$  regardless of whether the most  
245 coastal stations (G and T) were included in the statistical analysis ( $S=31917$ ,  $p<0.001$ ,  $r^2=0.44$ ,  $n=70$ ) or not  
246 ( $S=25985$ ,  $p<0.01$ ,  $r^2=0.35$ ,  $n=62$ ) (Fig. 3d).

247 Cell-specific degradation rates of DHAA increased with depth and yielded significantly higher rates at the lower  
248 oxycline compared to all shallower depths ( $n_{\text{bottom\_low\_hypoxic}}=6$ ,  $n_{\text{remaining depths}}=56$ ,  $W=302$ ,  $p<0.01$ ). Cell-specific  
249 GLUCase degradation rate and LAPase and GLUCase  $V_{\text{max}}$  showed the same patterns (Fig. 4g-j)

### 250 3.3. Bacterial contribution to the loss of dissolved organic carbon and oxygen in the 251 oxycline

252 We calculated the loss of oxygen and DOC during physical transport from below the mixed layer depth (MLD; 10-  
253 32 m) to 60 m based on observed changes in diapycnal fluxes (Eq. (1), Fig. 5). We estimated the bacterial  
254 contribution to this loss with two different assumptions (Table 1): i) We assumed that the loss of DOC over depth  
255 can be solely attributed to bacterial uptake implying that the DOC is subsequently incorporated as bacterial biomass  
256 (bacterial production) or respired to  $\text{CO}_2$  (Eq. (2)). ii) For the second approach the amount of DOC taken up by  
257 bacteria was determined by the measured bacterial incorporation of carbon (bacterial production) and a constant ratio  
258 between carbon that is taken up and carbon that is incorporated as biomass (bacterial production) (Eq. (3)). This ratio  
259 (BGE), was here assumed to be between 10 and 30%, based on the empirical equation by Rivkin and Legendre with  
260 an *in situ* temperature that varied between 14 and 19°C (Rivkin and Legendre, 2001).

261 For total average DOC loss ( $\nabla\Phi_{\text{DOC}}$ ), we calculated a range of 1.13-3.40  $\text{mmol C m}^{-3} \text{d}^{-1}$ , with loss rates decreasing  
262 most strongly below the shallow mixed layer down to 40 m (Table 1, Fig. 5). Following the first (i) assumption all  
263 DOC that was lost over depth was taken up by bacteria and the measured bacterial production represents the fraction





264 of DOC that was incorporated as biomass. Consequently, the remaining DOC that has been taken up, in other words  
265 the difference between DOC loss and bacterial production ( $0.01\text{-}0.29 \text{ mmol C m}^{-3} \text{ d}^{-1}$ ), was respired to  $\text{CO}_2$  and  
266 represents the bacterial oxygen demand to account for the DOC loss ( $\text{BOD}_\epsilon$ ) ( $1.05\text{-}3.38 \text{ mmol O}_2 \text{ m}^{-3} \text{ d}^{-1}$ ) (Eq. (2)).  
267 Following this calculation, the BGE would vary between 0.5-8.6% and 1.1-7.0% in the depth range of MLD-40 m  
268 and 40-60 m, respectively, being on average constant over the two different depth ranges (2.7%). ii) Applying a BGE  
269 in the range of 10-30% and the measured bacterial production, the calculated bacterial DOC uptake was  $0.04\text{-}2.9$   
270  $\text{mmol C m}^{-3} \text{ d}^{-1}$ . Hence, respiration of DOC to  $\text{CO}_2$  accounted for a  $\text{BOD}_\phi$  of  $0.03\text{-}2.63 \text{ mmol O}_2 \text{ m}^{-3} \text{ d}^{-1}$  (Table 1).

#### 271 4. Discussion

272 We investigated bacterial degradation of dissolved organic matter by measuring bacterial production rates as an  
273 estimate for organic carbon transformation into biomass as well as rates of extracellular hydrolytic enzymes to  
274 provide information on the initial steps of organic matter degradation (Hoppe et al., 2002). We expected reduced  
275 rates of organic matter degradation within oxygen depleted waters, since anaerobic respiration has a lower energy  
276 yield than aerobic respiration. However, although bacterial production decreased with depth (Fig. 3b), this decrease  
277 was not related to oxygen concentrations. Moreover, no significant increase in bacterial production was observed at  
278 the lower oxycline, when oxygen increased again (Fig. 3b). Decreasing bacterial production with depth has also been  
279 observed for fully oxygenated regions in the Atlantic (Baltar et al., 2009) and the equatorial Pacific (Kirchman et al.,  
280 1995) and has been explained by a decrease in the amount of bioavailable organic matter over depth.

281 The hypothesis of reduced bacterial degradation activity within the OMZ implies reduced extracellular enzyme rates  
282 for the hydrolysis of organic matter. In our study, neither GLUCase nor LAPase  $V_{\max}$  were reduced within the  
283 suboxic waters irrespective of incubation conditions (Fig. 4d, e, supplementary Fig. 1c, d). Thus, our findings show  
284 no evidence for reduced organic matter degradation in suboxic waters and are in good agreement with studies, which  
285 report similar bacterial degradation rates for oxic and suboxic waters (Cavan et al., 2017; Lee, 1992; Pantoja et al.,  
286 2009). Consequently, the hypothesis of enhanced carbon export in suboxic and anoxic waters due to reduced organic  
287 matter degradation seems fragile and alternative explanations for enhanced carbon export efficiency in suboxic and  
288 anoxic waters e.g. reduced particle fragmentation due to zooplankton avoiding hypoxia (Cavan et al., 2017) may be  
289 more likely. Moreover, a reduced degradation of organic matter in suboxic waters as it is assumed for particulate  
290 carbon in global ocean biogeochemical modelling may have to be reconsidered (Ilyina et al., 2013).

291 Within OMZs dissolved nitrogen fuels e.g. denitrification or anaerobic ammonium oxidation (anammox) and is  
292 reduced to e.g. dinitrogen gas, nitrous oxide that evades to the atmosphere. Current estimates result in 20-50% of the  
293 total oceanic nitrogen loss occurring in OMZs (Lam and Kuypers, 2011). Thereby, a preferential degradation of  
294 amino acid containing organic matter in suboxic waters compared to oxic waters has been suggested (Van Mooy et  
295 al., 2002). A strong degradation of nitrogen compounds (within suboxic waters) by heterotrophic bacteria (e.g.  
296 denitrifiers) enables the release of ammonia and nitrite and subsequently can maintain anammox, an autotrophic  
297 anaerobic respiratory pathway (Lam and Kuypers, 2011; Ward, 2013). This interaction between denitrifiers and



298 anammox bacteria would further fuel the loss of nitrogen to the atmosphere. Our data indeed showed enhanced  
299 degradation of amino acid containing organic matter in low oxygen waters. Indicators for protein decomposition, i.e.  
300 LAPase  $V_{\max}$  and the degradation rate of DHAA by LAPase, were more pronounced within the suboxic waters (Fig.  
301 4b, d). The close coupling between anammox and denitrifying bacteria has previously been shown for wastewater  
302 treatments. There, denitrifiers directly utilize organic matter excreted by the anammox bacteria which in turn benefit  
303 from the released nitrite by respiratory nitrate reduction (Lawson et al., 2017). In the Pacific, denitrifiers and  
304 anammox bacteria coexist, but are separated in space and time (Dalsgaard et al., 2012), therefore their inter-  
305 dependency is probably weaker than in waste water treatments. Still, high protein hydrolysis rates within suboxic  
306 waters might fuel enhanced nitrogen loss due to the mutual support of anammox bacteria and heterotrophic  
307 denitrifiers.

308 To investigate physiological effects of suboxia, we normalized bacterial production and enzymatic rates to cell  
309 abundance and found higher cell-specific bacterial production near the oxycline compared to suboxic waters and  
310 highest cell-specific enzyme rates at the lower oxycline (Fig. 3d, 4 g-j). Higher cell-specific bacterial production at  
311 oxic-anoxic interfaces in the water column has previously been reported for the Baltic Sea (Brettar et al., 2012).  
312 Baltar et al. (2009) showed increasing cell-specific enzymatic rates and decreasing cell-specific bacterial production,  
313 with increasing depth in the subtropical Atlantic and related this pattern to decreasing organic matter lability. Besides  
314 organic matter lability, TDN might influence physiological rates and was increasing with depth (Fig. 2c). We  
315 therefore suggest that the co-occurrence of oxygen and high TDN near the oxyclines favours (micro) aerobic  
316 respiration (Kalvelage et al., 2015) and cell activity, corroborating highly active bacterial communities at oxyclines.

317 Depth distribution of cell-specific and total bacterial production was markedly different (Fig. 3b, d) and can be  
318 explained by higher cell abundance (Fig. 3c) partially compensating for the lower metabolic activity in the OMZ  
319 core. The reduced cell-specific production in the core of the OMZ points to either a high standing stock of bacteria  
320 with low activity or a mixed community of less active and more active cells. One reason for the accumulation of cells  
321 within the OMZ might be that some bacterivores tend to avoid the OMZ Anderson et al. (2012), highlighting the  
322 OMZ core as an ecological niche for slowly growing bacteria.

323 In general, bacterial community composition in OMZs has been shown to be strongly impacted by oxygen. In the  
324 OMZ near the shelf off Chile Arctic96BD-19 and SUP05 dominate heterotrophic and autotrophic groups in hypoxic  
325 waters (Aldunate et al., 2018). Next to the appearance of autotrophic bacteria that are related to sulphur (e.g. SUP05)  
326 or nitrogen cycling (e.g. Planctomycetes) also bacteria that are related to cycling of complex carbohydrates have  
327 been discovered in OMZs (Callbeck et al., 2018; Galán et al., 2009; Thrash et al., 2017), and may explain the  
328 unaltered high potential ( $V_{\max}$ ) of the extracellular enzymes GLUCase and heterotrophic bacterial production in  
329 suboxic waters in our study (Fig. 4e, 3b). For instance, SAR406, SAR202, ACD39 and PAUC34f have the genetic  
330 potential for the turnover of complex carbohydrates and anaerobic respiratory processes, in the Gulf of Mexico  
331 (Thrash et al., 2017).

332 Heterotrophic bacteria are the main users of marine dissolved organic matter (Azam et al., 1983; Carlson and  
333 Hansell, 2015) and responsible for ~79% of total respiration in the Pacific Ocean (Del Giorgio et al., 2011),



334 proposing that heterotrophic bacteria drive organic matter and oxygen cycling in the ocean and significantly  
335 contribute to the formation of the OMZ. Under the assumption that the calculated loss of DOC during diapycnal  
336 transport (<60 m) is caused solely by bacterial uptake and subtracting the amount of carbon channelled into biomass  
337 production, our study verifies the importance of bacterial DOC degradation for the formation of the OMZ. We  
338 estimated a BOD ( $1.05\text{-}3.38 \text{ mmol O}_2 \text{ m}^{-3} \text{ d}^{-1}$ ) that is in line with earlier respiration measurements in the upper  
339 oxycline off Peru (Kalvelage et al., 2015) and represents 19-33% of the oxygen loss over depth, implying a rather  
340 low average BGE (0.5-8.6%) (Table 1). Calculating the bacterial uptake of DOC from production rates and a more  
341 conservative BGE between 10 and 30% as previously suggested (Rivkin and Legendre, 2001) for the *in situ*  
342 temperature of 14 to 19 °C, 2-86% of the DOC loss and 0.4-26% of oxygen loss could be attributed to bacterial  
343 degradation of dissolved organic matter. Both approaches reveal a BGE that is still within the range of previous  
344 reports for upwelling systems of the Atlantic (<1-58%) or northeastern Pacific (<10%) (Alonso-Sáez et al., 2007; Del  
345 Giorgio et al., 2011). The high variability in BGE is a topic of ongoing research. Until now 54% of the variability  
346 could be explained by variations in temperature (Rivkin and Legendre, 2001). Our data suggest that oxygen  
347 availability may be another control of BGE leading to rather low BGE in low oxygen waters. This is especially  
348 indicated by a low and constant average BGE (2.6%), which we estimated for the water column down to 60m depth  
349 under the assumption that all DOC that is lost over depth can be attributed to bacterial uptake. A low BGE might be  
350 explained by a bacterial community that has higher energetic demands, but in return is adapted to variable oxygen  
351 conditions. Additionally, the BGE is decreasing with an increasing carbon to nitrogen ratio of the available substrate  
352 (Goldman et al., 1987). In the OMZ off Peru the ratio between DOC and dissolved organic nitrogen is frequently  
353 high (~12 to 16) (Loginova et al., 2018), and might further contribute to the low BGE. High respiration rates induced  
354 by bacterial DOC degradation contribute to sustaining the OMZ, besides oxygen consumption by bacteria that  
355 hydrolyze and degrade particulate organic matter (Cavan et al., 2017). Another, but likely minor contribution to  
356 overall respiration is made by zooplankton and higher trophic levels (e.g. Kiko et al., 2016). Additionally, physical  
357 processes such as an intrusion of oxygen depleted waters by eddies, upwelling or advection, may add to the oxygen  
358 and DOC loss over depth (Brandt et al., 2015; Llanillo et al., 2018; Steinfeldt et al., 2015).

359 Uncertainties of our assumption that the loss of DOC is caused solely by bacterial uptake include other processes  
360 potentially contributing to DOC removal, but not taken into consideration here like DOC adsorption onto particles,  
361 DOC uptake by eukaryotic cells or the physical coagulation of DOC into particles, e.g. by formation of gel-like  
362 particles such as transparent exopolymer particles and Coomassie stainable particles (Carlson and Hansell, 2015;  
363 Engel et al., 2004, 2005). Moreover, temporal variations in diapycnal fluxes may be large, as indicated by the  
364 confidence interval of solute fluxes (Fig. 5) during this study and by 2 to 10 times lower DOC and oxygen loss rates  
365 during other seasons (Loginova et al., 2018). However, our study is the first combining physical and microbial rate  
366 measurements for carbon and oxygen losses in the upwelling system off Peru and can help improving current  
367 biogeochemical models by constraining bacterial dissolved organic matter degradation.

368 In oxygen depleted waters of the Peruvian upwelling system, the chemoautotrophic process of anammox has been  
369 assumed to dominate anaerobic nitrogen cycling (Kalvelage et al., 2013), with lower but more constant rates  
370 compared to more sporadically occurring heterotrophic denitrification (Dalsgaard et al., 2012). Our study points



371 towards a widespread occurrence of heterotrophic denitrification processes in the Peruvian OMZ, since the here  
372 applied method for measuring bacterial production is restricted to heterotrophs. Our rates for bacterial production  
373 within the suboxic waters averaged to  $26 \mu\text{mol C m}^{-3} \text{ d}^{-1}$  ( $0.55\text{-}160 \mu\text{mol C m}^{-3} \text{ d}^{-1}$ ). To compare bacterial  
374 production, i.e. rate of carbon incorporation, with denitrification rates previously reported for the South Pacific  
375 (Dalsgaard et al., 2012; Kalvelage et al., 2013), we converted one mol of reduced nitrogen to 1.25 mol of oxidized  
376 carbon after the reaction equation given by Lam and Kuypers (2011). This calculation indicates that on average  $\leq 19$   
377  $\mu\text{mol C m}^{-3} \text{ d}^{-1}$  are oxidized by denitrifying bacteria in the Eastern Tropical Pacific (Dalsgaard et al., 2012; Kalvelage  
378 et al., 2013). Assuming a BGE of 20% (Del Giorgio and Cole, 1998) then suggests that denitrification supports a  
379 bacterial production of  $\leq 4 \mu\text{mol C m}^{-3} \text{ d}^{-1}$ , thus only about 15% of total heterotrophic bacterial production in suboxic  
380 waters determined in this study. For the sum of anaerobic carbon oxidation rates including denitrification, DNRA  
381 and simple nitrate reduction,  $109 \mu\text{mol C m}^{-3} \text{ d}^{-1}$  ( $6\text{-}515 \mu\text{mol C m}^{-3} \text{ d}^{-1}$ ) may be expected for the Peruvian shelf, with  
382 the reduction of nitrate to nitrite representing the largest proportion ( $2\text{-}505 \mu\text{mol C}^{-1} \text{ m}^{-3} \text{ d}^{-1}$ ), based on the relative  
383 abundance of the different N-functional genes (Kalvelage et al., 2013). These anaerobic respiration measurements  
384 are equivalent to a bacterial production of  $\sim 22 \mu\text{mol C m}^{-3} \text{ d}^{-1}$  ( $1\text{-}103 \mu\text{mol C m}^{-3} \text{ d}^{-1}$ ) and are thus in good agreement  
385 with our direct measurements of bacterial production rates. However, the reduction of nitrate, could not be detected  
386 at every depth and incubation experiments partly showed huge variations over depth (Kalvelage et al., 2013),  
387 whereas we were able to measure bacterial production in every sample. Our data therefore suggest that the carbon  
388 oxidation potential off Peru is more evenly distributed than expected and also corroborate earlier suggestions of  
389 unexpectedly high rates of heterotrophic nitrogen cycling in the OMZ off Peru based on observations of high  
390 concentrations of atmospheric nitrous oxide (Bourbonnais et al., 2017).

## 391 **5. Conclusion**

392 Our study suggests that suboxia does not reduce enzymatic degradation of organic matter and bacterial production in  
393 the Eastern Tropical South Pacific off Peru. Bacterial production in suboxic waters points towards a dominance of  
394 heterotrophic anaerobic respiratory pathways, and may fuel high nitrogen loss rates to the atmosphere including  
395 climate relevant nitrous oxide as previously observed for this system. Clear differences between cell-specific and  
396 total rates of bacterial activity allude to different controls of cell abundance in suboxic systems and highlight the  
397 OMZ as a specific ecological niche. The combination of bacterial and physical rate measurements suggests that low  
398 BGEs in the upper oxycline contribute to sustaining the OMZ. Our study highlights the need for a better  
399 understanding and quantification of processes responsible for oxygen and dissolved organic matter loss in OMZs that  
400 is inevitable to predict future patterns of deoxygenation in a warming climate.

401 *Data Availability.* PANGAEA: 10.1594/PANGAEA.891247

402

403 *Author contributions.* M.M. and A.E. designed the scientific study, analysed the data and wrote the manuscript. J.L.  
404 calculated DOC and oxygen fluxes, G.K. sampled and calibrated the CTD data and both helped writing the  
405 manuscript.



406 *Competing interests.* The authors declare that they have no conflict of interest.

407 *Acknowledgments:* We thank Jon Roa, Tania Klüver and Ruth Flerus for the sampling and/or analysis of DOC/TDN;  
408 cell abundance, bacterial production and DHAA. Moreover, we would like to thank Judith Piontek, Sören Thomsen,  
409 Carolina Cisternas-Novoa and Frédéric A.C. Le Moigne who helped and gave advice for sampling during the cruises.  
410 We are grateful to the working group of Hermann Bange and Stefan Sommer who provided Winkler measurements.  
411 We thank the cruise leaders Hermann Bange and Marcus Dengler, crew, officers and the captains of the F.S. Meteor  
412 for the support on board and the successful cruises. This study was supported by the Helmholtz Association and by  
413 the Collaborative Research Center 754 / SFB Sonderforschungsbereich 754 ‘Climate-Biogeochemistry Interactions  
414 in the Tropical Ocean’.



415 **References**

- 416 Aldunate, M., De la glesia, R., Bertagnolli, A. D. and Ulloa, O.: Oxygen modulates bacterial community composition  
417 in the coastal upwelling waters off central Chile, *Deep. Res. Part II*, in press, 1–12, doi:10.1016/j.dsr2.2018.02.001,  
418 2018.
- 419 Alonso-Sáez, L., Gasol, J. M., Arístegui, J., Vilas, J. C., Vaqué, D., Duarte, C. M. and Agustí, S.: Large-scale  
420 variability in surface bacterial carbon demand and growth efficiency in the subtropical northeast Atlantic Ocean,  
421 *Limnol. Oceanogr.*, 52(2), 533–546, doi:10.4319/lo.2007.52.2.0533, 2007.
- 422 Anderson, R., Winter, C. and Jürgens, K.: Protist grazing and viral lysis as prokaryotic mortality factors at Baltic Sea  
423 oxic–anoxic interfaces, *Mar. Ecol. Prog. Ser.*, 467, 1–14, doi:10.3354/meps10001, 2012.
- 424 Azam, F., Fenchel, T., Field, J. G., Gray, J. S., Meyer-Reil, L. A. and Thingstad, F.: The ecological role of water-  
425 column microbes in the sea., *Mar. Ecol. Prog. Ser.*, 10(3), 257–263, 1983.
- 426 Baltar, F., Arístegui, J., Sintes, E., van Aken, H. M., Gasol, J. M. and Herndl, G. J.: Prokaryotic extracellular  
427 enzymatic activity in relation to biomass production and respiration in the meso- and bathypelagic waters of the  
428 (sub)tropical Atlantic, *Environ. Microbiol.*, 11(8), 1998–2014, doi:10.1111/j.1462-2920.2009.01922.x, 2009.
- 429 Benner, R. and Amon, R. M. W.: The size-reactivity continuum of major bioelements in the ocean, *Ann. Rev. Mar.*  
430 *Sci.*, 7(1), 185–205, doi:10.1146/annurev-marine-010213-135126, 2015.
- 431 Boetius, A. and Lochte, K.: Effect of organic enrichments on hydrolytic potentials and growth of bacteria in deep-sea  
432 sediments., *Mar. Ecol. Prog. Ser.*, 140, 239–250, doi:10.3354/meps140239, 1996.
- 433 Bourbonnais, A., Letscher, R. T., Bange, H. W., Échevin, V., Larkum, J., Mohn, J., Yoshida, N. and Altabet, M. A.:  
434 N<sub>2</sub>O production and consumption from stable isotopic and concentration data in the Peruvian coastal upwelling  
435 system, *Global Biogeochem. Cycles*, 31(4), 678–698, doi:10.1002/2016GB005567, 2017.
- 436 Brandt, P., Bange, H. W., Banyte, D., Dengler, M., Didwischus, S., Fischer, T., Greatbatch, R. J., Hahn, J., Kanzow,  
437 T., Karstensen, J., Körtzinger, A., Krahnemann, G., Schmidtke, S., Stramma, L., Tanhua, T. and Visbeck, M.: On the  
438 role of circulation and mixing in the ventilation of oxygen minimum zones with a focus on the eastern tropical North  
439 Atlantic, *Biogeosciences*, 12, 489–512, doi:10.5194/bg-12-489-2015, 2015.
- 440 Brettar, I., Christen, R. and Höfle, M. G.: Analysis of bacterial core communities in the central Baltic by comparative  
441 RNA–DNA-based fingerprinting provides links to structure–function relationships., *ISME J.*, 6(1), 195–212,  
442 doi:10.1038/ismej.2011.80, 2012.
- 443 Callbeck, C. M., Lavik, G., Ferdelman, T. G., Fuchs, B., Gruber-vodicka, H. R., Hach, P. F., Littmann, S.,  
444 Schöffelen, N. J., Kalvelage, T., Thomsen, S., Schunck, H., Löscher, C. R., Schmitz, R. A. and Kuypers, M. M. M.:  
445 Oxygen minimum zone cryptic sulfur cycling sustained by offshore transport of key sulfur oxidizing bacteria, *Nat.*



- 446 Commun., 9(1729), 1–11, doi:10.1038/s41467-018-04041-x, 2018.
- 447 Carlson, C. A. and Hansell, D. A.: DOM Sources, Sinks, Reactivity, and Budgets, in *Biogeochemistry of Marine*  
448 *Dissolved Organic Matter*, pp. 65–126, Elsevier., 2015.
- 449 Cavan, E. L., Trimmer, M., Shelley, F. and Sanders, R.: Remineralization of particulate organic carbon in an ocean  
450 oxygen minimum zone, *Nat. Commun.*, 8(May 2016), 14847, doi:10.1038/ncomms14847, 2017.
- 451 Cole, J. J. and Pace, M. L.: Bacterial secondary production in oxic and anoxic freshwaters, *Limnol. Oceanogr.*, 40(6),  
452 1019–1027, doi:10.4319/lo.1995.40.6.1019, 1995.
- 453 Czeschel, R., Stramma, L., Schwarzkopf, F. U., Giese, B. S., Funk, A. and Karstensen, J.: Middepth circulation of  
454 the eastern tropical South Pacific and its link to the oxygen minimum zone, *J. Geophys. Res.*, 116(C01015), 1–13,  
455 doi:10.1029/2010JC006565, 2011.
- 456 Dalsgaard, T., Thamdrup, B., Farías, L. and Revsbech, N. P.: Anammox and denitrification in the oxygen minimum  
457 zone of the eastern South Pacific, *Limnol. Oceanogr.*, 57(5), 1331–1346, doi:10.4319/lo.2012.57.5.1331, 2012.
- 458 Derek H. Olge: *FSA: Fisheries Stock Analysis*, 2018.
- 459 Devol, A. H. and Hartnett, H. E.: Role of the oxygen-deficient zone in transfer of organic carbon to the deep ocean,  
460 *Limnol. Oceanogr.*, 46(7), 1684–1690, doi:10.4319/lo.2001.46.7.1684, 2001.
- 461 Dittmar, T., Cherrier, J. and Ludichowski, K. U.: The analysis of amino acids in seawater., in *Practical guidelines for*  
462 *the analysis of seawater.*, edited by O. Wurl, pp. 67–78, CRC Press, Boca Raton., 2009.
- 463 Engel, A. and Galgani, L.: The organic sea-surface microlayer in the upwelling region off the coast of Peru and  
464 potential implications for air–sea exchange processes, *Biogeosciences*, 13(4), 989–1007, doi:10.5194/bg-13-989-  
465 2016, 2016.
- 466 Engel, A. and Händel, N.: A novel protocol for determining the concentration and composition of sugars in  
467 particulate and in high molecular weight dissolved organic matter (HMW-DOM) in seawater., *Mar. Chem.*, 127(1),  
468 180–191, doi:10.1016/j.marchem.2011.09.004, 2011.
- 469 Engel, A., Thoms, S., Riebesell, U., Rochelle-Newall, E. and Zondervan, I.: Polysaccharide aggregation as a  
470 potential sink of marine dissolved organic carbon, *Nature*, 428(6986), 929–932, doi:10.1038/nature02453, 2004.
- 471 Engel, A., Zondervan, I., Aerts, K., Beaufort, L., Benthien, A., Chou, L., Delille, B., Gattuso, J.-P., Harlay, J.,  
472 Heemann, C., Hoffmann, L., Jacquet, S., Nejtgaard, J., Pizay, M.-D., Rochelle-Newall, E., Schneider, U.,  
473 Terbruggen, A. and Riebesell, U.: Testing the direct effect of CO<sub>2</sub> concentration on a bloom of the coccolithophorid  
474 *Emiliania huxleyi* in mesocosm experiments, *Limnol. Oceanogr.*, 50(2), 493–507, doi:10.4319/lo.2005.50.2.0493,  
475 2005.



- 476 Fischer, T., Banyte, D., Brandt, P., Dengler, M., Krahnemann, G., Tanhua, T. and Visbeck, M.: Diapycnal oxygen  
477 supply to the tropical North Atlantic oxygen minimum zone, *Biogeosciences*, 10(7), 5079–5093, doi:10.5194/bg-10-  
478 5079-2013, 2013.
- 479 Galán, A., Molina, V., Thamdrup, B., Woebken, D., Lavik, G., Kuypers, M. M. M. and Ulloa, O.: Anammox bacteria  
480 and the anaerobic oxidation of ammonium in the oxygen minimum zone off northern Chile, *Deep. Res. II*, 56, 1021–  
481 1031, doi:10.1016/j.dsr2.2008.09.016, 2009.
- 482 Gasol, J. M. and Del Giorgio, P. A.: Using flow cytometry for counting natural planktonic bacteria and  
483 understanding the structure of planktonic bacterial communities, *Sci. Mar.*, 64(2), 197–224,  
484 doi:10.3989/scimar.2000.64n2197, 2000.
- 485 Del Giorgio, P. A. and Cole, J. J.: Bacterial growth efficiency in natural aquatic systems, *Annu. Rev. Ecol. Syst.*,  
486 29(May), 503–541, 1998.
- 487 Del Giorgio, P. A., Condon, R., Bouvier, T., Longnecker, K., Bouvier, C., Sherr, E. and Gasol, J. M.: Coherent  
488 patterns in bacterial growth, growth efficiency, and leucine metabolism along a northeastern Pacific inshore-offshore  
489 transect, *Limnol. Oceanogr.*, 56(1), 1–16, doi:10.4319/lo.2011.56.1.0001, 2011.
- 490 Goldman, J. C., Caron, D. A. and Dennett, M. R.: Regulation of gross growth efficiency and ammonium regeneration  
491 in bacteria by substrate C : N ratio., *Limnol. Oceanogr.*, 32(6), 1239–1252, doi:10.4319/lo.1987.32.6.1239, 1987.
- 492 Graco, M. I., Purca, S., Dewitte, B., Castro, C. G., Morón, O., Ledesma, J., Flores, G. and Gutiérrez, D.: The OMZ  
493 and nutrient features as a signature of interannual and low-frequency variability in the Peruvian upwelling system,  
494 *Biogeosciences*, 14(20), 4601–4617, doi:10.5194/bg-14-4601-2017, 2017.
- 495 Grossart, H., Allgaier, M., Passow, U. and Riebesell, U.: Testing the effect of CO<sub>2</sub> concentration on the dynamics of  
496 marine heterotrophic bacterioplankton, *Limnol. Oceanogr.*, 51(1), 1–11, doi:10.4319/lo.2006.51.1.0001, 2006.
- 497 Gruber, N.: Warming up, turning sour, losing breath : ocean biogeochemistry under global change., *Philos. Trans. R.  
498 Soc.*, 369(1943), 1980–1996, doi:10.1098/rsta.2011.0003, 2011.
- 499 Hadley Wickham: *ggplot2: Elegant Graphics for Data Analysis*, Springer-Verlag, New York., 2016.
- 500 Hoppe, H.-G.: Significance of exoenzymatic activities in the ecology of brackish water: measurements by means of  
501 methylumbelliferyl-substrates., *Mar. Ecol. Prog. Ser.*, 11, 299–308, 1983.
- 502 Hoppe, H.-G., Gocke, K. and Kuparinen, J.: Effect of H<sub>2</sub>S on heterotrophic substrate uptake, extracellular enzyme  
503 activity and growth of brackish water bacteria., *Mar. Ecol. Prog. Ser.*, 64, 157–167 [online] Available from:  
504 <http://www.int-res.com/articles/meps/64/m064p157.pdf>, 1990.
- 505 Hoppe, H.-G., Arnosti, C. and Herndl, G. F.: Ecological significance of bacterial enzymes in the marine  
506 environment, in *Enzymes in the environment: activity, ecology, and applications*, edited by R. Burns and R. Dick,





- 507 pp. 73–108, Marcel Dekker, Inc., New York., 2002.
- 508 Horthorn, T., Bretz, F. and Westfall, P.: Simultaneous Inference in General Parametric Models, *Biometrical J.*, 50(3),  
509 346–363, 2008.
- 510 Ilyina, T., Six, K. D., Segschneider, J., Maier-Reimer, E., Li, H. and Nunez-Riboni, I.: Global ocean biogeochemistry  
511 model HAMOCC : Model architecture and performance as component of the MPI-Earth system model in different  
512 CMIP5 experimental realizations, *J. Adv. Model. earth Syst.*, 5, 1–29, doi:10.1029/2012MS000178, 2013.
- 513 John Fox and Sanford Weisberg: *An {R} Companion to Applied Regression*, 2nd ed., SAGE Publications Ltd,  
514 Thousand Oak {CA}., 2011.
- 515 Kalvelage, T., Lavik, G., Lam, P., Contreras, S., Arteaga, L., Löscher, C. R., Oschlies, A., Paulmier, A., Stramma, L.  
516 and Kuypers, M. M. M.: Nitrogen cycling driven by organic matter export in the South Pacific oxygen minimum  
517 zone, *Nat. Geosci.*, 6(3), 228–234, doi:10.1038/ngeo1739, 2013.
- 518 Kalvelage, T., Lavik, G., Jensen, M. M., Revsbech, N. P., Löscher, C., Schunck, H., Desai, D. K., Hauss, H., Kiko,  
519 R., Holtappels, M., LaRoche, J., Schmitz, R. A., Graco, M. I. and Kuypers, M. M. M.: Aerobic microbial respiration  
520 in oceanic oxygen minimum zones, edited by Z.-X. Quan, *PLoS One*, 10(7), e0133526,  
521 doi:10.1371/journal.pone.0133526, 2015.
- 522 Kämpf, J. and Chapman, P.: *Upwelling Systems of the World*, Springer International Publishing Switzerland, Cham.  
523 [online] Available from: <http://link.springer.com/10.1007/978-3-319-42524-5>, 2016.
- 524 Kiko, R., Hauss, H., Buchholz, F. and Melzner, F.: Ammonium excretion and oxygen respiration of tropical  
525 copepods and euphausiids exposed to oxygen minimum zone conditions, *Biogeoscience*, 13, 2241–2255,  
526 doi:10.5194/bg-13-2241-2016, 2016.
- 527 Kirchman, D., K'nees, E. and Hodson, R.: Leucine incorporation and its potential as a measure of protein synthesis  
528 by bacteria in natural aquatic systems., *Appl. Environm. Microbiol.*, 49(3), 599–607, 1985.
- 529 Kirchman, D. L., Rich, J. H. and Barber, R. T.: Biomass and biomass production of heterotrophic bacteria along  
530 140°W in the equatorial Pacific: Effect of temperature on the microbial loop, *Deep Sea Res. Part II Top. Stud.*  
531 *Oceanogr.*, 42(2–3), 603–619, doi:10.1016/0967-0645(95)00021-H, 1995.
- 532 Lam, P. and Kuypers, M. M. M.: Microbial nitrogen cycling processes in oxygen minimum zones., *Annu. Rev. Mar.*  
533 *Sci.*, 3, 317–348, doi:10.1146/annurev-marine-120709-142814, 2011.
- 534 Lawson, C. E., Wu, S., Bhattacharjee, A. S., Hamilton, J. J., McMahon, K. D., Goel, R. and Noguera, D. R.:  
535 Metabolic network analysis reveals microbial community interactions in anammox granules., *Nat. Commun.*,  
536 8(15416), 1–12, doi:10.1038/ncomms15416, 2017.
- 537 Lee, C.: Controls on organic carbon preservation : the use of stratified water bodies to compare intrinsic rates of



- 538 decomposition in oxic and anoxic systems., *Geochim. Cosmochim. Acta*, 56(8), 3323–3335, doi:10.1016/0016-  
539 7037(92)90308-6, 1992.
- 540 Lindroth, P. and Mopper, K.: High performance liquid chromatographic determination of subpicomole amounts of  
541 amino acids by precolumn fluorescence derivatization with o-phthaldialdehyde., *Anal. Chem.*, 51(11), 1667–1674,  
542 doi:10.1021/ac50047a019, 1979.
- 543 Llanillo, P. J., Pelegrí, J. L., Talley, L. D., Pena-Izquierdo, J. and Cordero, R. R.: Oxygen Pathways and Budget for  
544 the Eastern South Pacific Oxygen Minimum Zone, *J. Geophys. Res.*, 123, 1722–1744, doi:10.1002/2017JC013509,  
545 2018.
- 546 Loginova, A. N., Thomsen, S., Dengler, M., Lüdke, J. and Engel, A.: Diapycnal dissolved organic matter supply into  
547 the upper Peruvian oxycline, *Biogeosciences Discuss.*, 2(June), 1–23, doi:10.5194/bg-2018-284, 2018.
- 548 McDougall, T. J. and Barker, P. M.: Getting started with TEOS-10 and the Gibbs Seawater (GSW) oceanographic  
549 toolbox, SCOR/IAPSO WG 127, , 28, 2011.
- 550 Van Mooy, B. A. S., Keil, R. G. and Devol, A. H.: Impact of suboxia on sinking particulate organic carbon:  
551 Enhanced carbon flux and preferential degradation of amino acids via denitrification., *Geochim. Cosmochim. Acta*,  
552 66(3), 457–465, doi:10.1016/S0016-7037(01)00787-6, 2002.
- 553 Pantoja, S., Rossel, P., Castro, R., Cuevas, L. A., Daneri, G. and Córdova, C.: Microbial degradation rates of small  
554 peptides and amino acids in the oxygen minimum zone of Chilean coastal waters, *Deep Sea Res. Part*, 56(16), 1055–  
555 1062, doi:10.1016/j.dsr2.2008.09.007, 2009.
- 556 Piontek, J., Sperling, M., Nöthig, E. M. and Engel, A.: Regulation of bacterioplankton activity in Fram Strait (Arctic  
557 Ocean) during early summer: The role of organic matter supply and temperature., *J. Mar. Syst.*, 132, 83–94,  
558 doi:10.1016/j.jmarsys.2014.01.003, 2014.
- 559 R Development Core Team: R: A language and environment for statistical computing, [online] Available from:  
560 <http://www.r-project.org>, 2008.
- 561 Rivkin, R. B. and Legendre, L.: Biogenic carbon cycling in the upper ocean: Effects of microbial respiration, *Science*  
562 , 291(5512), 2398–2400, doi:10.1126/science.291.5512.2398, 2001.
- 563 Roullier, F., Berline, L., Guidi, L., Durrieu De Madron, X., Picheral, M., Sciandra, A., Pesant, S. and Stemmann, L.:  
564 Particle size distribution and estimated carbon flux across the Arabian Sea oxygen minimum zone, *Biogeosciences*,  
565 11(16), 4541–4557, doi:10.5194/bg-11-4541-2014, 2014.
- 566 Schafstall, J., Dengler, M., Brandt, P. and Bange, H.: Tidal-induced mixing and diapycnal nutrient fluxes in the  
567 Mauritanian upwelling region, *J. Geophys. Res.*, 115(C10), C10014, doi:10.1029/2009JC005940, 2010.
- 568 Schlitzer, R.: *Ocean Data View*, 2016.



- 569 Simon, M. and Azam, F.: Protein content and protein synthesis rates of planktonic marine bacteria., *Mar. Ecol. Prog.*  
570 *Ser.*, 51(3), 201–213, 1989.
- 571 Smith, D. C. and Azam, F.: A simple , economical method for measuring bacterial protein synthesis rates in seawater  
572 using <sup>3</sup>H-leucine, *Mar. Microb. Food Web*, 6(2), 107–114, 1992.
- 573 Steinfeldt, R., Sültenfuß, J., Dengler, M., Fischer, T. and Rhein, M.: Coastal upwelling off Peru and Mauritania  
574 inferred from helium isotope disequilibrium, *Biogeoscience*, 12, 7519–7533, doi:10.5194/bg-12-7519-2015, 2015.
- 575 Stramma, L., Schmidtko, S., Levin, L. A. and Johnson, G. C.: Ocean oxygen minima expansions and their biological  
576 impacts, *Deep Sea Res. Part I Oceanogr. Res. Pap.*, 57(4), 587–595, doi:10.1016/j.dsr.2010.01.005, 2010.
- 577 Sugimura, Y. and Suzuki, Y.: A high-temperature catalytic oxidation method for the determination of non-volatile  
578 dissolved organic carbon in seawater by direct injection of a liquid sample, *Mar. Chem.*, 24(2), 105–131,  
579 doi:10.1016/0304-4203(88)90043-6, 1988.
- 580 Taylor, G. T., Thunell, R., Varela, R., Benitez-Nelson, C. and Scranton, M. I.: Hydrolytic ectoenzyme activity  
581 associated with suspended and sinking organic particles within the anoxic Cariaco Basin, *Deep Sea Res. I*, 56(8),  
582 1266–1283, doi:10.1016/j.dsr.2009.02.006, 2009.
- 583 Thamdrup, B., Dalsgaard, T. and Revsbech, N. P.: Widespread functional anoxia in the oxygen minimum zone of the  
584 Eastern South Pacific, *Deep Sea Res. Part I Oceanogr. Res. Pap.*, 65, 36–45, doi:10.1016/j.dsr.2012.03.001, 2012.
- 585 Thrash, C. J., Seitz, K. W., Baker, B. J., Temperton, B., Gillies, L. E., Rabalais, N. N., Henrissat, B. and Mason, U.:  
586 Metabolic roles of uncultivated bacterioplankton lineages in the northern Gulf of Mexico “Dead Zone,” *MBio*, 8(5),  
587 1–20, doi:10.1128/mBio.01017-17, 2017.
- 588 Ward, B. B.: How nitrogen is lost, *Science* ., 341(6144), 352–353, doi:10.1126/science.1240314, 2013.
- 589 Weiss, M., Abele, U., Weckesser, J., Welte, W., Schiltz, E. and Schulz, G.: Molecular architecture and electrostatic  
590 properties of a bacterial porin, *Science* ., 254(5038), 1627–1630, doi:10.1126/science.1721242, 1991.
- 591 Winkler, W. L.: Die Bestimmung des im Wasser gelösten Sauerstoffes., *Berichte der Dtsch. Chem. Gesellschaft*,  
592 21(2), 2843–2854, doi:10.1002/cber.188802102122, 1888.
- 593



594 **Figure legends**

595

596 **Figure 1:** Station map. All presented stations in the Eastern Tropical South Pacific off Peru sampled in 2017. For detailed  
597 informations about the stations see supplementary Table 1.

598 **Figure 2:** Biotic and abiotic conditions at selected stations exemplary for the sampling conditions. Chlorophyll (a), temperature  
599 (b), total dissolved nitrogen (TDN) (c), dissolved organic carbon (DOC) (d), carbon content of dissolved hydrolysable amino  
600 acids (DHAA) (e) and carbon content of high molecular weight dissolved carbohydrates (DCHO) (f) over depth at different  
601 stations from on- to offshore off Peru.

602

603 **Figure 3:** Bacterial growth activity at different *in situ* oxygen concentrations from on- to offshore off Peru. Oxygen  
604 concentrations (a), total bacterial production (BP) (b), bacterial abundance (c) cell-specific BP (d) over the upper 800 m depth  
605 with a zoom in the upper 100 m (small plots).

606

607 **Figure 4:** Extracellular enzyme rates at different *in situ* oxygen concentrations. Oxygen concentrations (a), degradation rates of  
608 dissolved amino acids (DHAA) by leucine-aminopeptidase (LAPase) (b), degradation rates of high molecular weight dissolved  
609 carbohydrates (DCHO) by  $\beta$ -glucosidase (GLUCase) (c) total potential LAPase rates ( $V_{max}$ ) (d), Glucose  $V_{max}$  (e), cell abundance  
610 (f), cell-specific degradation rates DHAA by LAPase (g), cell-specific degradation rates of DCHO by GLUCase (h), cell-specific  
611 LAPase  $V_{max}$  (i) and cell-specific Glucose  $V_{max}$  (j) at different oxygen regimes off Peru.

612

613 **Figure 5:** Measured concentrations and calculated proxies for the change of dissolved organic carbon (DOC) and dissolved  
614 oxygen (DO) flux over depth for stations G-T: The average diapycnal diffusivity of mass ( $K_\rho$ ) over depth with confidence interval  
615 and the constant  $K_\rho (1 \times 10^{-3} m^2 s^{-1})$  that was used for further calculations (a). Concentrations of DOC in the upper 100 m and  
616 the resulting change of DOC flux over depth ( $\mathcal{F}\Phi$ ) (b). Concentrations of DO in the upper 100 m and the resulting change of DO  
617 flux over depth ( $\mathcal{F}\Phi$ ) (c).

618

619



620 **Tables**

621 **Table 1:** Estimates of oxygen and DOC loss over depth based on *in situ* physical observations and bacterial rate measurements. Oxygen and DOC loss rates were estimated from the  
 622 change in oxygen and DOC fluxes over depth. The bacterial uptake of DOC was calculated from bacterial production based on a growth efficiency of 10 and 30% (DOC uptake<sub>φ</sub>). The  
 623 bacterial oxygen demand (BOD) and bacterial growth efficiency (BGE<sub>ε</sub>) was calculated from bacterial production and the assumption that DOC loss can be completely explained by  
 624 bacterial uptake (BOD<sub>ε</sub>) or estimated based on a BGE of 10 and 30% (BOD<sub>φ</sub>).

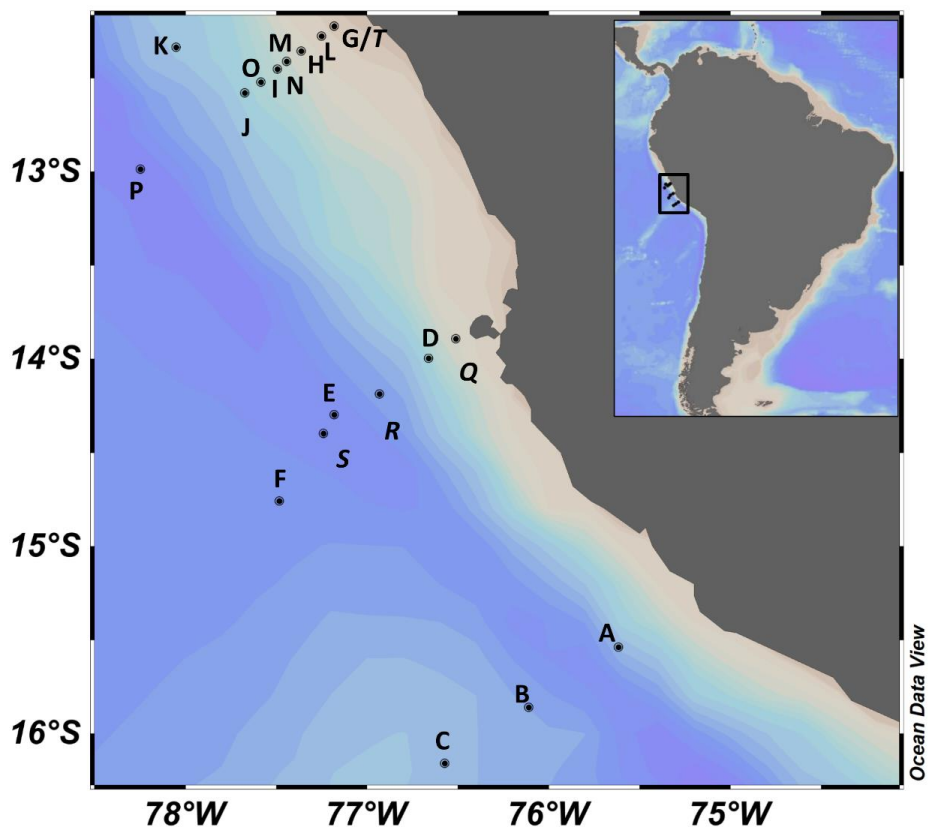
625

Depth	oxygen loss	DOC loss	DOCuptake <sub>φ10</sub>			DOC uptake <sub>φ30</sub>			Bacterial Production			BOD <sub>ε</sub>			BOD <sub>φ10</sub>			BOD <sub>φ30</sub>			BGE <sub>ε</sub>								
[m]	[mmol m <sup>-3</sup> d <sup>-1</sup> ]																		%										
	avg	avg	avg	min	max	avg	min	max	avg	min	max	avg	min	max	avg	min	max	avg	min	max	avg	min	max	avg	min	max			
MLD-40	10.23	3.4	0.90	0.17	2.92	0.30	0.06	0.97	0.09	0.02	0.29	3.3	3.1	3.38	0.81	0.15	2.63	0.21	0.04	0.68	2.65	0.50	8.62						
40-60	5.55	1.13	0.30	0.12	0.79	0.10	0.04	0.26	0.03	0.01	0.08	1.1	1.05	1.12	0.27	0.11	0.72	0.07	0.03	0.19	2.67	1.10	7.04						

626



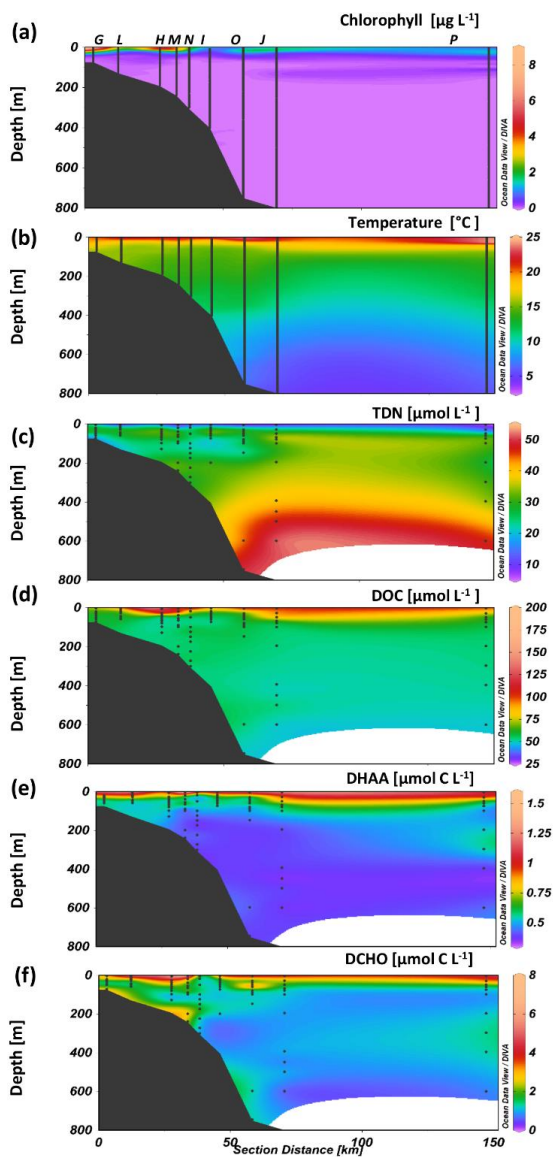
627 **Figures**



628

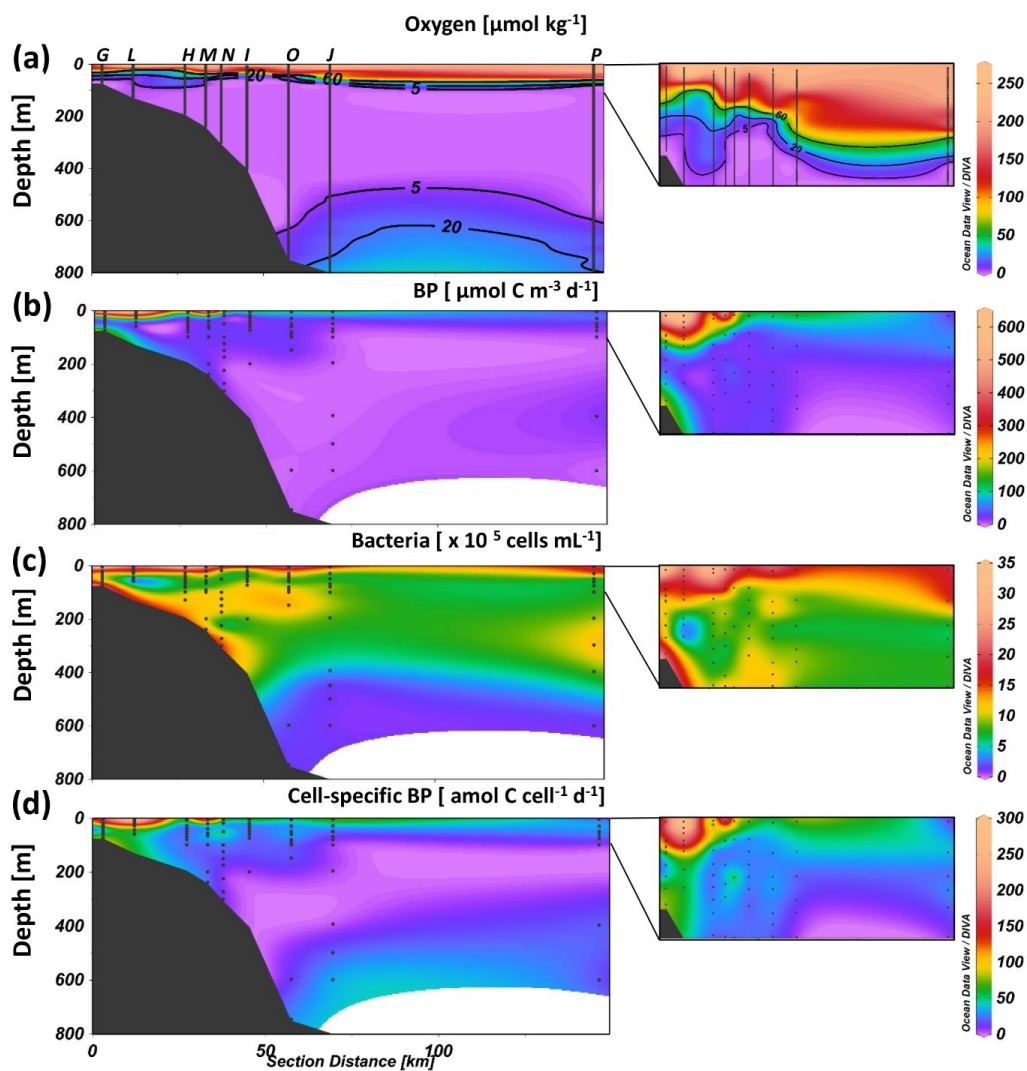
629 **Figure 1**

630



631

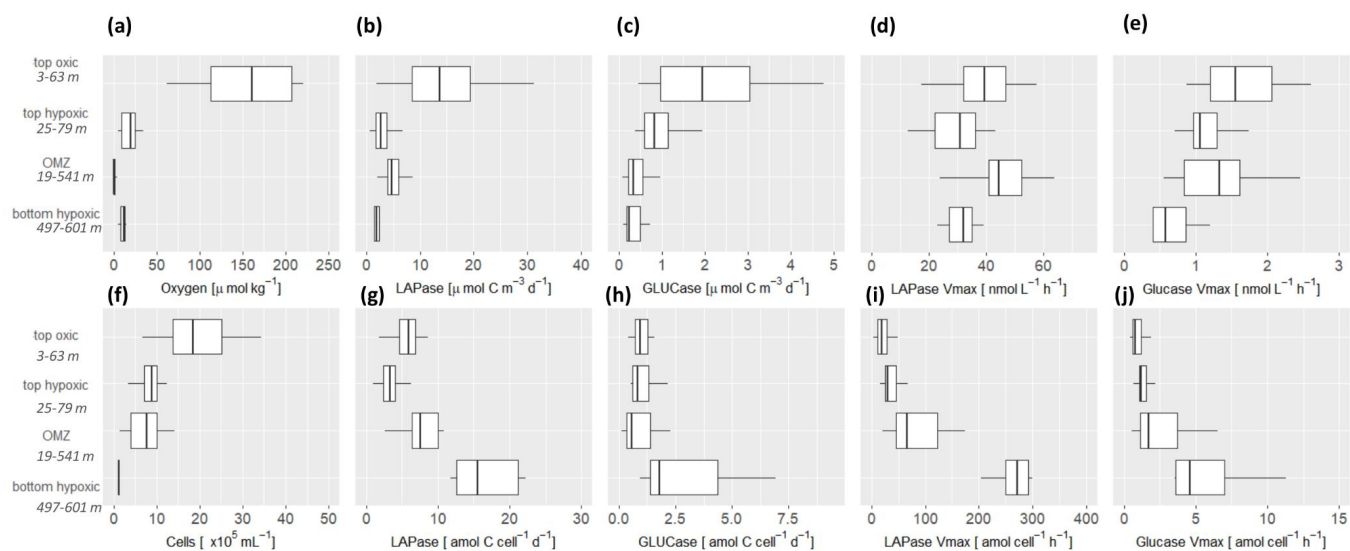
632 **Figure 2**



633

634 **Figure 3**





635

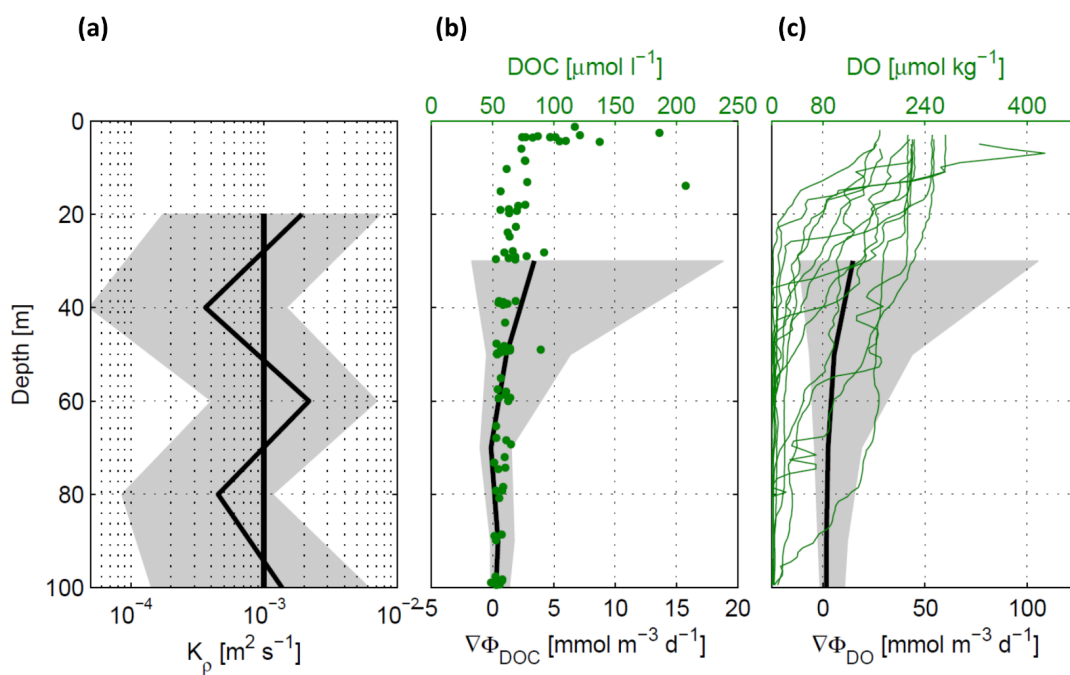
636 **Figure 4**

637

638

639

640



641

642

643

644 **Figure 5**